

Fast Micro-Kelvin Resolution Thermometer Based on NTC Thermistors

Franz E. Wudy,[†] Dominik J. Moosbauer,[†] Michael Multerer,[‡] Georg Schmeer,[†] Hans-Georg Schweiger,[†] Christoph Stock,[§] Peter F. Hauner,[†] Gottfried A. Suppan,[†] and Heiner J. Gores^{*,†,§}

[†]Institute of Physical and Theoretical Chemistry, University of Regensburg, 93053 Regensburg, Germany

[‡]Zahner-elektrik GmbH & Co. KG, 96317 Kronach, Germany

[§]Institute of Physical Chemistry, Westfälische Wilhelmsuniversität, 48149 Münster, Germany

ABSTRACT: Thermometers with temperature resolutions of equal or better than 1 mK typically make use of platinum wire temperature sensors such as the PT100. Alternating current techniques to read out these fairly low dynamic temperature sensors are complex and expensive and act slowly. This work shows that it is possible to build up a thermometer with even higher resolution up to 75 μ K, capable of delivering a data-rate of up to ten readouts per second by means of negative temperature coefficient sensors. We selected the measurement of two binary solid–liquid phase diagrams (biphenyl/naphthalene and biphenyl/benzophenone) to check the presented equipment.

INTRODUCTION

Examinations of chemical reaction kinetics, thermodynamic parameters, and physical phenomena often call for high temperature resolutions. In the past many efforts have been made to achieve those high quality temperature data, for example, Beckmann thermometers, several kinds of digital thermometers, and even thermometers that determine changes in oscillation frequencies of a quartz crystal or other kinds of resonators.¹ We present here a digital approach using a precision semiconductor temperature sensor to build up a thermometer that delivers high quality thermal data.

MATERIALS AND METHODS

Temperature Sensor. The thermistor 30K6A1A (BetaTHERM Corporation, Shresbury, MA, U.S.A.) finds use as a temperature sensor in our setups. BetaTHERM denotes this type of thermistor as “interchangeable”, meaning one sensor can be replaced by another thermistor without having significant changes in temperature readouts. Significant changes, in this case, are supposed to not exceed 0.1 K. As a consequence, BetaTHERM propagates these thermistors as a possible replacement for the defacto industrial standard PT100.² In fact, modern thermistors do not deserve their bad reputation with respect to their initial and long-term stabilities. Sydenham and Collins³ observed stabilities in the magnitude of $\pm 200 \mu$ K/1000 h, a stability of 30 mK within six months was found by us,⁴ and BetaTHERM itself specifies the stability with 0.097 K over 9 years at a constant storage temperature of 75 °C.⁵ New methods of cutting and handling semiconductor materials⁶ and improvements in the microstructure, as well as in-factory premature aging processes, render these stabilities possible.

On top of this, the electric resistance of thermistors shows a huge dynamic response with respect to changes in temperature, in comparison with the above-mentioned PT100 platinum resistor sensor. Within a Celsius temperature range from (–100 to +100) °C, the resistance of the 30K6A1A thermistor R_T varies over 3 orders of magnitude, whereas PT100 resistors show in its

resistance (R_{PT100}) a variation of only approximately 100 Ω , see Figure 1 for comparison with respect to the Celsius temperature Θ . Large negative temperature coefficients can be determined⁷ for thermistors. As for their negative temperature coefficients, these sensors are named NTC resistors as well. Another advantage over the PT100 sensors is the outstanding small dimension of about 3 mm diagonally, not only resulting in practical mechanical manageability in narrow places but also in very fast response characteristics.

Electronic Setup. In the past mainly alternating current (AC) bridges, so-called Kohlrausch-bridges, have been used and still find use in the field for metrological detection of temperature. These setups mostly consist of precision resistor decades, sine voltage generators, and lock-in amplifiers with magnitude and phase detectors, capacitance cancellation units, and thermal compensation networks to detect the resistance of PT100 sensors. Even though Unni et al. recently have shown⁸ that such a setup can show impressive long-term stabilities ($\pm 45 \mu$ K/h), during the past decade semiconductor manufacturers have improved direct current (DC) techniques in a way that AC techniques do not necessarily dominate any longer. BetaTHERM’s 30K6A1A has a resistance of about 30 k Ω at a temperature of 25 °C. Such a high resistance and the high temperature coefficient suggest going without such a bridge circuitry. Instead, a simple voltage divider circuit as shown in Figure 2 can be built up.

The voltage divider is formed by the NTC resistor R_T and a special precision resistor R_{prc} (100 k $\Omega \pm 0.1\%$, CMF 0805, SRT Resistor Technology, Cadolzburg, Germany) with a very low temperature coefficient of only 5 ppm/K. The voltage divider is driven with an ultrastable reference voltage of 5 V $\pm 0.2\%$ (U_{ref} 3 ppm/K) over its rails. This high-resistance layout entails a

Special Issue: Kenneth N. Marsh Festschrift

Received: July 26, 2011

Accepted: October 4, 2011

Published: October 20, 2011

heat dissipated power of only $40 \mu\text{W}$ at $25 \text{ }^\circ\text{C}$ within the thermistor.

At the center point of the voltage divider the resulting signal is filtered slightly by means of the capacitor C28 to remove high-frequency noise. Figure 3 shows the resistance of the NTC as well as the voltage at the voltage divider as a function of Celsius temperature Θ . The voltage signal is processed by an operational amplifier (OP) in impedance converter configuration (IC9A) and filtered actively using a Sallen-Key filter⁹ which is set up with IC9A, R2, R3, C26, and C27 to have unity-gain Butterworth low-pass characteristics. R13 and C42 form an additional low-pass filter and a charge reservoir for the following analog to digital converter (ADC). The filter's -3 dB_V (70 %) attenuation is at 4.3 Hz; at 50 Hz the filter shows an attenuation of -46.5 dB_V (20 ppm), the overall filter has a slope of about -40 dB_V per decade. As the filter capacitors have connection to the thermometer's electrical ground plane, leakage currents have to be avoided, as they falsify the measurement. Consequently film-type capacitors with very low leakage currents are used; the MKS-02 capacitors supplied by Wima (Mannheim, Germany) are supposed to have very high-value parasitic parallel resistances in the order

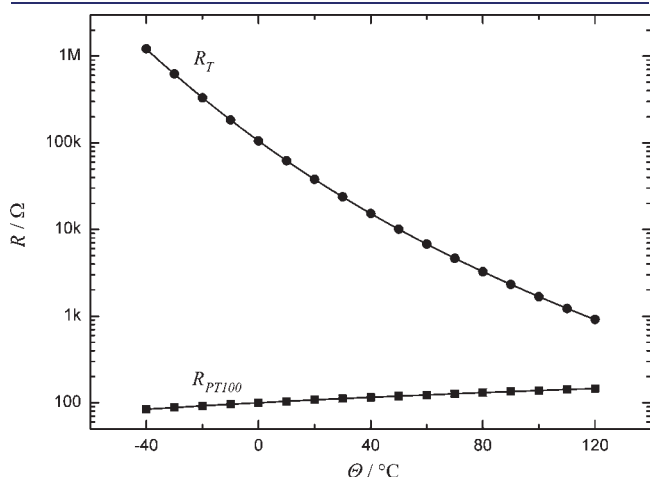


Figure 1. Thermistor 30K6A1A (with electrical resistance R_T) and a typical PT100 platinum-wire sensor (R_{PT100}) are compared by their resistance behavior between $\Theta = (-40 \text{ and } +120) \text{ }^\circ\text{C}$.

of $10 \text{ G}\Omega$ and more so that these falsifications can be neglected. OPs are selected particularly for DC characteristics for the thermometer. The OP AD8629 (Analog Devices, Norwood, MA, U.S.A.) has a very low input offset voltage of about $1.0 \mu\text{V}$ and a very low offset voltage drift of 2 nV/K and introduces nearly no noise. The noise voltage is on the order of $0.5 \mu\text{V}$ from peak to peak. This setup of voltage divider and filter is repeated four times in a highly symmetrical way so that a four channel thermometer is set up in total.

The four channel ADC ADS1234 (Texas Instruments, Dallas, TX, U.S.A.) converts these analog voltages into digital information with 24 bit resolution, from which 21.4 bit are supposed to be noise-free,¹⁰ so that the ADC is able to detect voltages with a resolution of $0.4 \mu\text{V}$. The ADC itself includes a digital low-pass filter, which suppresses (additionally to the analog filter) noise at frequencies of 50, 60, 100, and 120 Hz with an attenuation exceeding -150 dB_V . The ADC can record up to 10 measurement points per second.

The ADC, as well as the USB data connection to a computer, and a Liquid Crystal Display are controlled by a 32 bit ARM7 microprocessor. As the thermometer is supplied with power via the USB interface, complex filtering mechanisms have to take

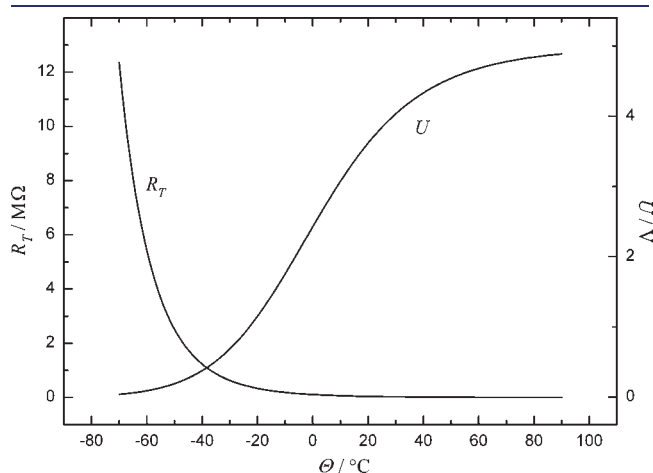


Figure 3. Electrical resistance of the thermistor R_T and the voltage at the voltage divider U plotted vs the Celsius temperature Θ .

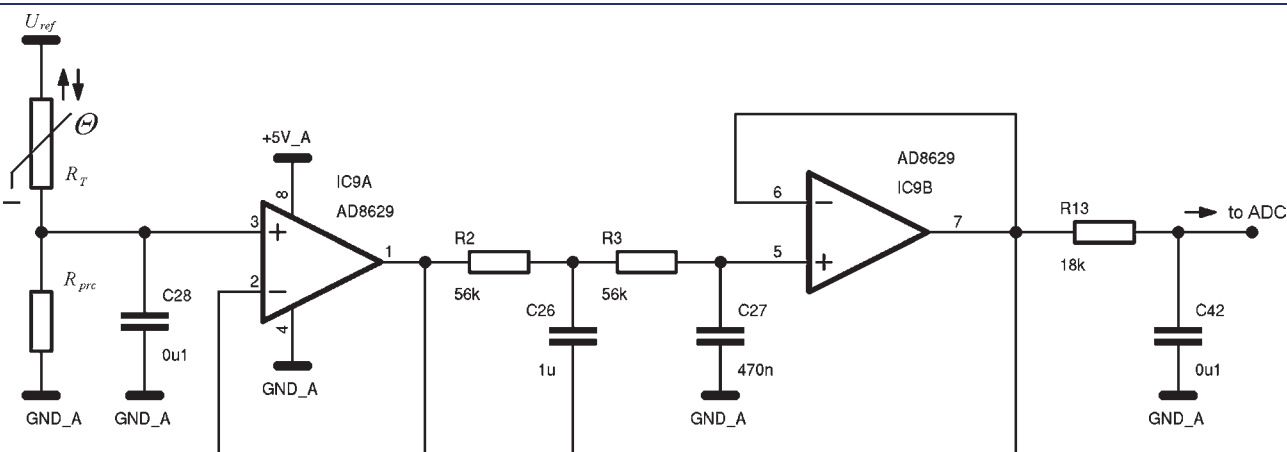


Figure 2. Thermistor 30K6A1A (R_T) and the precision resistor R_{prec} form a voltage divider. The voltage signal is filtered afterward at unity gain. For details see the electronic setup.

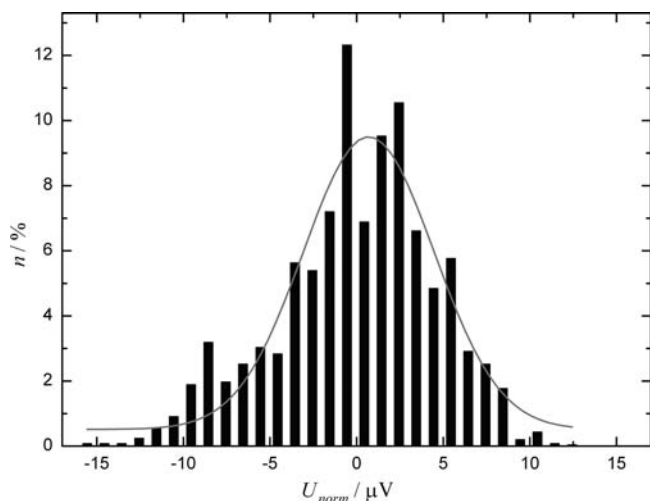


Figure 4. Histogram showing a typical frequency distribution of the ADC counts n in percentages referred to normalized voltages U_{norm} .

place. The analog part of the thermometer is even built up with a floating ground to avoid any ground loops and electrical interferences.

The electronic parts are housed inside an aluminum case with small dimensions of $100 \times 100 \times 60$ mm. The Liquid Crystal Display is installed at the front side. At the reverse side USB connector, earth connection receptacle and four push–pull connectors for attaching the thermistors are placed.

The thermometer's data stream is processed at the host computer using a user-friendly program written in optimized C code. Data can be stored locally into a text file or into a SQL database system.

Noise. To detect the real resolution of the thermometer via the signal-to-noise level, four low-noise precision resistors are connected to the thermometer instead of NTC sensors. The ADC data of the four channels were collected for two hours and subjected to statistical tests; compare Figure 4 for a histogram of the measured voltages U_{norm} with the relative frequency of observations n . The standard deviation of the mean value provides information on the voltage noise level, in this case about $4 \mu\text{V}$. This value is only ten times higher than the ADC's maximum noise-free resolution ($0.4 \mu\text{V}$) renders possible.

Transfer Function. As the thermometer basically determines the voltage at the voltage divider, this information has to be converted into the thermistor's resistance and then into the temperature. To calculate the resistance of the thermistor, the voltage divider equation can be used

$$U = U_{\text{ref}} \frac{R_{\text{prc}}}{R_{\text{prc}} + R_{\text{T}}} \quad (1)$$

U denotes the voltage at the voltage divider related to the ultrastable reference voltage U_{ref} with respect to the precision resistor's resistance R_{prc} and the temperature-dependent resistance of the thermistor R_{T} .

Several methods to calculate the temperature from the thermistor's resistance are known. A thermodynamic description for an ideal semiconductor can be used

$$\frac{R_{\text{T}}}{R_{\text{N}}} = \exp \left[\frac{E_{\text{A}}}{k_{\text{B}}} \left(\frac{1}{T} - \frac{1}{T_{\text{N}}} \right) \right] \quad (2)$$

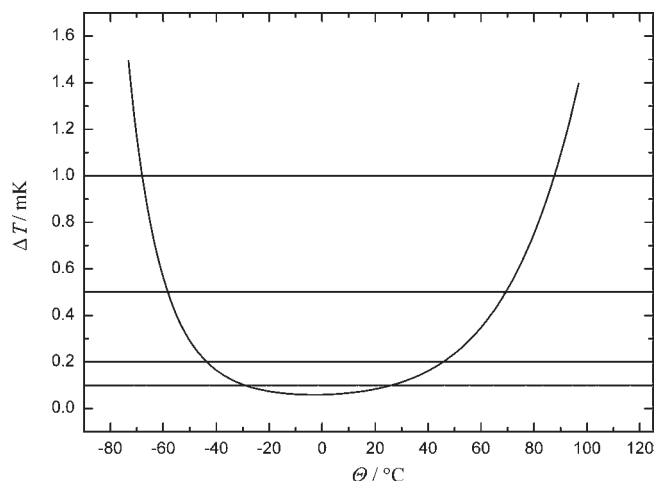


Figure 5. Temperature-dependent resolution ΔT of the thermometer.

R_{T} describes the resistance at the absolute temperature T , R_{N} is the nominal resistance at a nominal temperature T_{N} , E_{A} is the material-specific activation energy, and k_{B} is Boltzmann's constant.

A more accurate but empirical approach is represented by the Steinhart–Hart equation¹¹

$$\frac{1}{T} = A + B \ln \frac{R_{\text{T}}}{R_0} + C \left(\ln \frac{R_{\text{T}}}{R_0} \right)^3 \quad (3)$$

with $R_0 = 1 \Omega$ and A , B , and C are the intrinsic factors that can be determined via calibration. For low-precision measurements, factors specified by the manufacturer can be used instead.

Temperature Resolution. Equations 1 and 3 and the already known noise voltage of the thermometer ($4 \mu\text{V}$) can be used to calculate the thermometer's temperature resolution ΔT which depends on temperature, as it is shown in Figure 5 for the Celsius scale. In the temperature range (-30 to $+30$) $^{\circ}\text{C}$, the resolution is better than $100 \mu\text{K}$; the highest resolution can be achieved at about $-5 \text{ }^{\circ}\text{C}$ with a value of $75 \mu\text{K}$. In the range (-70 to $+90$) $^{\circ}\text{C}$ the resolution tends to be not above 1 mK .

Precision. Temperature is defined by the international temperature scale, restated 1990 (ITS-90),^{12,13} based mostly on triple points and phase transition points of pure elements and compounds. These points can only be determined with a limited accuracy. As we only have water triple-point cells in our laboratories, we decided to calibrate our thermometer against a thermometer (ASL, U.K., Precision Thermometer F250 MKII, $\pm 0.005 \text{ K}$) with a PT100 temperature sensor and a valid calibration certificate. Up to now platinum resistance thermometers have been the standard thermometers which can be calibrated by national and international institutes of standards. Hence statements on precision¹⁴ in this article are not referenced to any reference points of the ITS-90 but to the thermometer which was used for the calibration task.

In practice, the temperature sensor of the reference thermometer and the glass-encapsulated thermistors are tempered in a precision thermostat¹⁵ capable of maintaining temperatures with a deviation of only 1 mK . The reference thermometer records reference temperatures Θ_{ref} and the herein introduced thermometer records voltages U at the voltage divider. Over the time t this calibration process has been recorded.

Data sets are processed to remove outliers and to calculate mean values. The (U/V , $\Theta_{\text{ref}}/^{\circ}\text{C}$) data-pairs are fitted on the

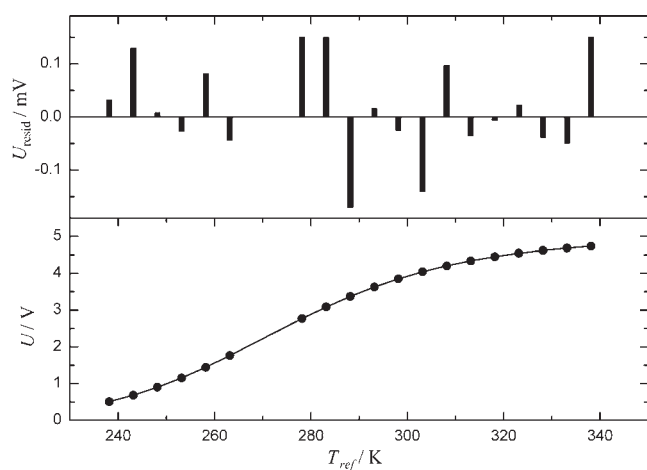


Figure 6. Calibration process. Discrete voltage values U as a function of absolute temperatures T_{ref} (●) are fitted on eq 4. The behavior of the residual voltage U_{resid} is shown on top.

following equation to determine the parameters A , B , and C :

$$U = \frac{R_{\text{prc}} U_{\text{ref}}}{R_{\text{prc}} + R_0 \exp\left(S - \frac{B}{3C\xi}\right)}$$

$$S = \left(\zeta - \frac{1}{2\xi}\right)^{1/3}$$

$$\zeta = \sqrt{\frac{1}{27} \frac{B^3}{C^3} + \frac{1}{4}\xi^2} \quad (4)$$

$$\xi = \frac{A - \frac{1}{T_{\text{ref}}}}{C}$$

$$T_{\text{ref}} = 273.15 \text{ K} + \Theta_{\text{ref}} \frac{\text{K}}{^\circ\text{C}}$$

This equation can be obtained by solving eq 3 for R_T and inserting into eq 1. Figure 6 shows a typical plot of gathered (U_{resid}/V , T_{ref}/K) data-pairs and the data fit.

Typically, a residual analysis yields an error of about 100 μV . Analog to the noise analysis, the precision of the thermometer with respect to the reference thermometer can be specified to 2.5 mK within (-30 to $+30$) $^\circ\text{C}$. Within (-70 and $+90$) $^\circ\text{C}$, the precision tends to be not below 25 mK. As the absolute precision of the reference thermometer is specified to be 30 mK, the overall error in absolute precision should not exceed 40 mK statistically. Nevertheless, the calibration process can improve the thermistors precision up to the factor 25, comparing 0.1 K precision with the factory parameters and 2.5 mK with the improved parameters. Calibration therefore is more than reasonable. For details of calibrating NTC sensors, see ref 4.

RESULTS AND DISCUSSION

We selected the measurement of two binary solid–liquid phase diagrams (biphenyl/naphthalene and biphenyl/benzophenone) to check the presented equipment. Biphenyl, naphthalene, and benzophenone obtained from Merck, Germany were purified by 2-fold sublimation before further use. The purity of each

Table 1. Molar Ratio x_{Biphenyl} , Melting Point Θ_{m} , and Eutectic Temperature Θ_{Eu} of the System Biphenyl/Naphthalene with Standard Deviations for at Least Three Measurements per Ratio at Pressure $p = 0.1 \text{ MPa}$ ^a

x_{Biphenyl}	$\Theta_{\text{m}}/^\circ\text{C}$	$\Theta_{\text{Eu}}/^\circ\text{C}$	$\Theta_{\text{m}}^{\text{lit}}/^\circ\text{C}$	$\Theta_{\text{Eu}}^{\text{lit}}/^\circ\text{C}$
0	80.00 ± 0.16		80.05^{17} , 80.26^{18} 80.28^{19}	
0.1250	71.95 ± 0.18	36.40 ± 0.37		
0.2500	63.63 ± 0.06	36.20 ± 0.35		
0.3750	54.18 ± 0.23	36.92 ± 0.05		
0.5000	41.00 ± 0.20	36.72 ± 0.18		
0.54				41.7^{16}
0.5600		36.73 ± 0.11		39.5^{17}
0.6250	45.92 ± 0.79	36.59 ± 0.55		
0.7000	52.04 ± 0.76	36.71 ± 0.11		
0.7500	56.04 ± 1.03	36.13 ± 0.30		
0.8750	62.90 ± 0.67	35.85 ± 0.39		
1	68.89 ± 0.23		69.0^{17} , 68.93^{18}	

^a Values of literature data for melting point $\Theta_{\text{m}}^{\text{lit}}$ and eutectic temperature $\Theta_{\text{Eu}}^{\text{lit}}$ are also shown. Standard uncertainty u is $u(p) = 30 \text{ kPa}$.

Table 2. Molar Ratio x_{Biphenyl} , Melting Point Θ_{m} , and Eutectic Temperature Θ_{Eu} of the System Biphenyl/Benzophenone at Pressure $p = 0.1 \text{ MPa}$ with Standard Deviations and Values in the Literature^a

x_{Biphenyl}	$\Theta_{\text{m}}/^\circ\text{C}$	$\Theta_{\text{Eu}}/^\circ\text{C}$	$\Theta_{\text{m}}^{\text{lit}}/^\circ\text{C}$	$\Theta_{\text{Eu}}^{\text{lit}}/^\circ\text{C}$
0	48.88 ± 1.22		47.7^{17} , 47.9^{18} 48.2^{20}	
0.1260	41.99 ± 0.12	18.82 ± 0.34		
0.1890	38.18 ± 1.38	18.72 ± 0.84		
0.2500	33.04 ± 1.04	18.73 ± 0.43		
0.3200	27.27 ± 0.88	17.81 ± 0.70		
0.3750		18.30 ± 0.32		
0.3930				25.2^{17}
0.4270	28.29 ± 0.21	18.13 ± 0.77		
0.5000	35.94 ± 0.57	18.73 ± 0.52		
0.6250	44.16 ± 0.11	18.12 ± 0.33		
0.7500	52.82 ± 0.08	17.52 ± 0.95		
0.8750	60.97 ± 0.65	18.55 ± 0.64		
1	68.89 ± 0.61		69.0^{17} , 68.93^{18}	

^a Standard uncertainty u is $u(p) = 30 \text{ kPa}$.

compound was checked via ^1H NMR spectroscopy. No impurities besides trace amounts of water were detected. Phase diagrams of binary organic systems containing biphenyl/naphthalene¹⁶ and biphenyl/benzophenone¹⁷ were determined by recording and evaluating the cooling curves with the presented device. The peripheral setup provided cooling rates up to 30 mK per second. With a data refreshment rate of 10 points every second and the precision higher 3 mK, every data pair of the curve was measured reliably. The compounds were weighed ($\pm 0.0001 \text{ g}$) to match the molar ratios given in Tables 1 and 2.

Each mixture was repeatedly heated to a temperature that was 15 $^\circ\text{C}$ above its visible melting point and subsequently cooled in order to get at least four data sets by recorded cooling curves for statistical treatment. This procedure was greatly simplified by

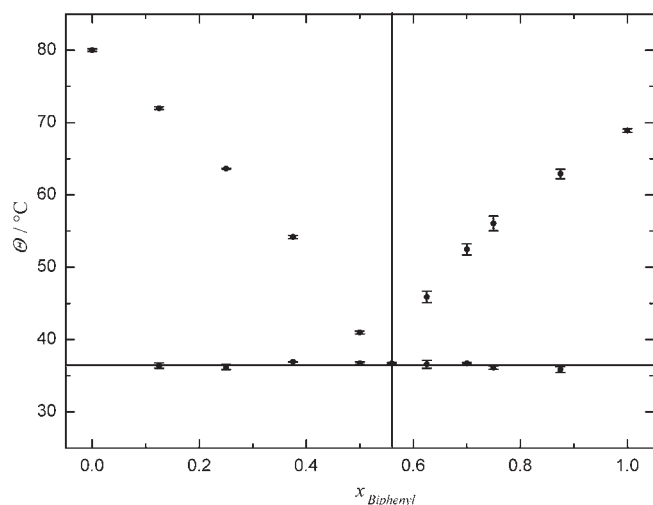


Figure 7. Binary melting point phase diagram of the eutectic system biphenyl/naphthalene.

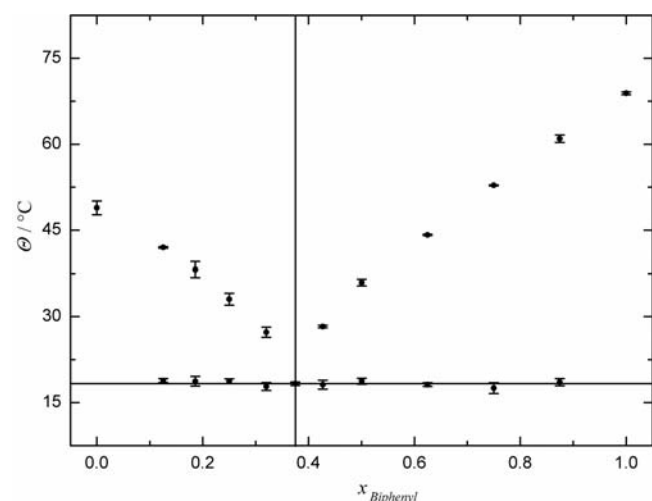


Figure 8. Binary melting point phase diagram of the eutectic system biphenyl/benzophenone.

recording the curves of four mixtures at the same time due to the thermometer's multichannel connection. For details of the evaluation of the cooling curves for determining equilibrium temperatures, see ref 21. The obtained diagrams of both systems are shown in Figures 7 and 8. The two phase diagrams show the excellent reliability of the thermometer. In nearly all mixtures especially the constancy of the eutectic temperature can be observed due to the accuracy and the fast response of the device. Because of its handiness and robustness the thermometer is suited for scientific experiments with high accuracy demands as it is for practical education as well.

CONCLUSION

The presented thermometer reaches a performance that is similar to that of commercially available precision thermometers. Commercial precision thermometers typically show a resolution of 1 mK and a data update rate of 0.3 Hz. The thermometer presented here exhibits a resolution of up to 75 μ K and a data refreshment rate of 10 Hz. A weight of only 400 g and the ultrasmall

footprint of only 100 \times 100 \times 60 mm make it attractive for use under small-sized requirements, e.g., glove boxes. A further non negligible advantage is its multichannel connection for simultaneously recording up to four temperatures. This thermometer can be produced at very low cost, as no customized hardware is needed. All parts can be bought off-the-shelf.

Because the main reason for this paper was to present a new thermometer with some outstanding properties, it is not useful to discuss the results of the phase diagrams in detail. Suffice it to note that despite Lee et al.¹⁷ used a thermometer with a precision of about 0.1 K only the results of this group are mainly in agreement with ours.

AUTHOR INFORMATION

Corresponding Author

*E-mail: heiner.gores@chemie.uni-regensburg.de; hgore_01@uni-muenster.de. Telephone: +49 941 943 4746. Fax: +49 941 943 4532.

Funding Sources

The Deutsche Forschungsgemeinschaft (DFG) in association with "Project Initiative PAK 177: Funktionsmaterialien und Materialanalytik zu Lithium-Hochleistungsbatterien (# 544243)" is gratefully acknowledged for financial support.

ACKNOWLEDGMENT

The authors thank B. C. Rodden (MRC Components OHG, Freising, Germany) and C. Collins (Betatherm Ireland Ltd., Galway, Ireland) for delivering a multiplicity of their 30K6A1A thermistors for experiments in our laboratories and W. Kühnl (SRT Resistor Technology GmbH, Cadolzburg, Germany) for making available precision resistors.

DEDICATION

Thanks to Ken Marsh for helpful discussions and motivating advices in the past. Thanks for improving our manuscripts submitted to the *Journal of Chemical Engineering Data*. Best wishes for his future.

REFERENCES

- (1) Hopcroft, M. A.; Kim, B.; Chandorkar, S.; Melamud, R.; Agarwal, M.; Jha, C. M.; Bahl, G.; Salvia, J.; Mehta, H.; Lee, H. K.; Candler, R. N.; Kenny, T. W. Using the temperature dependence of resonator quality factor as a thermometer. *Appl. Phys. Lett.* **2007**, *91* (1), No. 013505.
- (2) Monkman, G. Temperature measurement taken to extremes. *Sensor Rev.* **2001**, *21*, 177–181.
- (3) Sydenham, P. H.; Collins, G. C. Thermistor controller with microkelvin stability (for strainmeter testbase temperature control). *J. Phys. E: Sci. Instrum.* **1975**, *8*, 311–315.
- (4) Schweiger, H.-G.; Multerer, M.; Gores, H. J. Fast Multichannel Precision Thermometer. *IEEE Trans. Instrum. Meas.* **2007**, *56*, 2002–2009.
- (5) Zurbuchen, J. *Precision Thermistor Thermometry*. Measurement Science Conference Tutorial. Thermometry - Fundamentals And Practice, 1993. Available online: http://www.meas-spec.com/downloads/Precision_Thermistor_Thermometry.pdf (accessed May 2011).
- (6) Schaumburg, H. *Werkstoffe und Bauelemente der Elektrotechnik, Band 3: Sensoren*; BG Teubner: Leipzig, 1992.
- (7) Nicholas, J. V.; White, D. R. *Traceable Temperatures. An Introduction to Temperature Measurement and Calibration*, 2nd ed.; John Wiley: Chichester, U.K., 2001.

(8) Unni, P. K. M.; Gunasekaran, M. K.; Kumar, A. $\pm 30 \mu\text{K}$ temperature controller from 25 to 103 °C: Study and analysis. *Rev. Sci. Instrum.* **2003**, *74*, 231–242.

(9) Karki, J. *Analysis of the Sallen-Key architecture (Rev. B)*. Texas Instruments Application Report, 1999. Available online: <http://focus.ti.com/lit/an/sloa024b/sloa024b.pdf> (accessed May 2011).

(10) ADS1234. *24-Bit, Ultra Low-Noise Analog-to-Digital Converter*. Datasheet, Texas Instruments, 2008.

(11) Steinhart, J. S.; Hart, S. R. Calibration curves for thermistors. *Deep-Sea Res. Oceanogr. Abst.* **1968**, *15*, 497–503.

(12) Quinn, T. J. The international temperature scale of 1990 (ITS-90). *Phys. Scr.* **1990**, *41*, 730–732.

(13) McGlashan, M. L. The international temperature scale of 1990 (ITS-90). *J. Chem. Thermodyn.* **1990**, *22*, 653–663.

(14) Hans, V. High accuracy measuring method of absolute temperatures using thermistors. *Proceedings of the IEEE International Symposium on Industrial Electronics*, Xian, China, May 25–29, **1992**; 29–30.

(15) Barthel, J.; Buestrich, R.; Gores, H. J.; Schmidt, M.; Wuehr, M. A New Class of Electrochemically and Thermally Stable Lithium Salts for Lithium Battery Electrolytes. *J. Electrochem. Soc.* **1997**, *144*, 3866–3870.

(16) Gallus, J.; Lin, Q.; Zumbühl, A.; Friess, S. D.; Hartmann, R.; Meister, E. C. Binary Solid-Liquid Phase Diagrams of Selected Organic Compounds. A Complete Listing of 15 Binary Phase Diagrams. *J. Chem. Educ.* **2001**, *78*, 961–964.

(17) Lee, H. H.; Warner, J. C. The Systems (I) Diphenyl-Diphenylamine, (II) Diphenyl-Benzophenone and (III) Benzophenone-Diphenylamine. *J. Am. Chem. Soc.* **1933**, *55*, 209–214. Lee, H. H.; Warner, J. C. The System Biphenyl-Bibenzyl-Naphthalene. Nearly Ideal Binary and Ternary Systems. *J. Am. Chem. Soc.* **1935**, *57*, 318–321.

(18) Lide, D. R., Ed.; *CRC Handbook of Chemistry and Physics*, 90th ed.; CRC Press: Boca Raton, FL, 2010; (Internet Version 2010).

(19) McCullough, J. P.; Finke, H. L.; Messerly, J. F.; Todd, S. S.; Kincheloe, T. C.; Waddington, G. The Low-Temperature Thermodynamic Properties of Naphthalene, 1-Methylnaphthalene, 2-Methylnaphthalene, 1,2,3,4-Tetrahydronaphthalene, trans-Decahydronaphthalene and cis-Decahydronaphthalene. *J. Phys. Chem.* **1957**, *61*, 1105–1116.

(20) Rastogi, R. P.; Nigam, R. K.; Sharma, R. N.; Girdhar, H. L. Entropy of Fusion of Molecular Complexes. *J. Chem. Phys.* **1963**, *39*, 3042–3044.

(21) Wachter, P.; Schreiner, C.; Schweiger, H.-G.; Gores, H. J. Determination of phase transition points of ionic liquids by combination of thermal analysis and conductivity measurements at very low heating and cooling rates. *J. Chem. Thermodyn.* **2010**, *42*, 900–903.